blood®
Regular Article

HEMATOPOIESIS AND STEM CELLS

Aging alters the cell cycle control and mitogenic signaling responses of human hematopoietic stem cells

Colin A. Hammond,[1] Si Wei Wu,[1,2] Fangwu Wang,[1,2] Margarita E. MacAldaz,[1,2] and Connie J. Eaves[1-3]

[1]Terry Fox Laboratory, British Columbia Cancer Agency, Vancouver, Canada; and [2]Department of Medicine and [3]Department of Medical Genetics, The University of British Columbia, Vancouver, Canada

KEY POINTS

- Aging HSCs display a progressive and growth-factor sensitive elongation of G_1.
- Increased growth factor concentrations are required to stimulate mitogenesis in aging HSCs associated with reduced AKT activation.

Human hematopoietic stem cells (HSCs), like their counterparts in mice, comprise a functionally and molecularly heterogeneous population of cells throughout life that collectively maintain required outputs of mature blood cells under homeostatic conditions. In both species, an early developmental change in the HSC population involves a postnatal switch from a state in which most of these cells exist in a rapidly cycling state and maintain a high self-renewal potential to a state in which the majority of cells are in a quiescent state with an overall reduced self-renewal potential. However, despite the well-established growth factor dependence of HSC proliferation, whether and how this mechanism of HSC regulation might be affected by aging has remained poorly understood. To address this knowledge gap, we isolated highly HSC-enriched CD34$^+$CD38$^-$CD45RA$^-$CD90$^+$CD49f$^+$ (*CD49f$^+$*) cells from cord blood, adult bone marrow, and mobilized peripheral blood samples obtained from normal humans spanning 7 decades of age and then measured their functional and molecular responses to growth factor stimulation in vitro and their regenerative activity in vivo in mice that had undergone transplantation. Initial experiments revealed that advancing donor age was accompanied by a significant and progressively delayed proliferative response but not the altered mature cell outputs seen in normal older individuals. Importantly, subsequent dose-response analyses revealed an age-associated reduction in the growth factor–stimulated proliferation of *CD49f$^+$* cells mediated by reduced activation of AKT and altered cell cycle entry and progression. These findings identify a new intrinsic, pervasive, and progressive aging-related alteration in the biological and signaling mechanisms required to drive the proliferation of very primitive, normal human hematopoietic cells.

Introduction

Hematopoiesis is a hierarchically organized process that supports the lifelong production of many short-lived mature blood cells from a small number of cells with extensive self-sustaining ability. The stepwise changes that accompany and regulate this process at the single-cell level are now recognized to be complex and highly variable, even at a single developmental time point or from the same tissue source.[1] Aging in mice and humans alike is associated with a decreased output of mature lymphoid and red blood cells, an expansion of clones bearing leukemia-associated mutations (clonal hematopoiesis of indeterminate potential), and increased incidences of hematopoietic malignancies.[2-10] It is also well established that in aging mice there is a selective increase in hematopoietic stem cells (HSCs) that produce reduced outputs of mature B and T lymphocytes, despite retention of their repopulating activity and sustained outputs of other mature blood lineages in serial transplants.[11-16] Documented cell-intrinsic mechanisms of aging in mice include an observed accumulation of DNA damage, metabolic changes, and epigenetic alterations affecting HSC-specific functions.[4] More recent studies of cells from older humans have reported an aging-associated accumulation of cells with surface phenotypes variably enriched in functionally defined HSCs[17-20] but with a 5- to 40-fold decreased frequency of cells with mouse repopulating activity within the highly HSC-enriched CD34$^+$CD38$^-$CD45RA$^-$CD90$^+$CD49f$^+$ (*CD49f$^+$*) phenotype of cells in adult as compared with cord blood (CB) sources.[21-26]

Label-retention studies in mice have demonstrated that their HSCs are continuously, but infrequently, recruited from a quiescent state into cycle after 4 weeks of age, before which most are rapidly cycling.[27-31] A corresponding change in the cycling activity of HSCs in baboons and humans has been inferred to occur within the first 3 years of life based on the rate of telomere shortening exhibited by their short-lived neutrophil progeny.[32,33] In addition, the time required for maximally stimulated HSCs from young adult mice to complete a first division in vitro was found to correlate with the longevity of their

regenerative activity in vivo,[34] although this correlation was not found to extend to HSCs from aged mice.[35] In contrast, very little is known about how normal aging affects the properties of human HSCs for which inter-person variability is a major issue, numbers of highly-enriched phenotypes of functionally defined HSCs are much lower, and molecular heterogeneity has been revealed in single-cell analyses.[21,23,24,36-40]

Here, we report the results of a series of single-cell analyses of the initial kinetics of proliferation of *CD49f*$^+$ cells and their differentiated cell outputs in vitro and in vivo for cells from normal donors spanning 7 decades. The results reveal a progressive age-associated delay in progressing through the cell cycle coupled with desensitization of these cells to extrinsic mitogenic growth factors (GFs).

Methods

Primary sources of human cells

Anonymized heparinized samples of human blood and bone marrow (BM) samples from donors who were hematologically normal, aged between 0 and 69 years, were obtained and used in experiments with informed consent in accordance with the University of British Columbia Research Ethics Board approved protocols.

Flow cytometry and cell sorting

CD34$^+$ cells were isolated from fresh or thawed cells using EasySep and then suspended in Hanks balanced salt solution (STEMCELL Technologies) supplemented with 5% human serum (Millipore-Sigma) and 1.5 μg/mL antihuman CD32 antibody (clone IV.3; STEMCELL Technologies) and then stained with antibodies (supplemental Table 1, available on *Blood* website) for 1 to 2 hours on ice before analysis or fluorescence-activated cell sorting (FACS) on a FACSAria Fusion, FACSAria III sorter, or FACSymphony instrument (BD).

Stromal cell–containing cocultures

Individual *CD49f*$^+$ cells were index sorted into wells containing mixtures of mouse stromal cells producing human GFs supplemented with additional soluble GFs as previously described.[23] Cultures were maintained with weekly half-medium changes for 6 to 8 weeks as indicated after which clonal outputs were analyzed visually and when indicated for lymphocytes (B lineage and natural killer cells), neutrophils, and monocytes (NM cells; supplemental Tables 3 and 4). Clones were persistent if they remained until the end of the culture or assigned as transient if they were detectable at earlier time points but not at the end of the culture.

Xenotransplants

FACS-purified *CD49f*$^+$ cells were transplanted IV (either alone or in combination with 10^4 green fluorescent protein–labeled [GFP$^+$] CB cells) into sublethally irradiated 12- to 16-week-old female nonobese diabetic (NOD)-*Rag1*$^{-/-}$-*IL2Rγc*$^{-/-}$-*W*^{41}/*W*^{41} (NRG-W41) mice[41] (supplemental Tables 6 and 8). Human BM chimerism was assessed at weeks 4, 8, 12, 16, 20, and 30. Digital droplet polymerase chain reaction (ddPCR) was used to determine the extent to which the progeny of the GFP$^+$ cells might have contributed to the outputs attributed to the non-transduced (GFP$^-$) *CD49f*$^+$ cell–derived progeny.

Single-cell tracking

Single *CD49f*$^+$ cells were index sorted into Terasaki plates (Greiner) preloaded with serum-free medium (SFM) containing 10-fold dilutions of 300 ng/mL stem cell factor, 300 ng/mL FMS-like tyrosine kinase 3 ligand, and 60 ng/mL interleukin 3 (IL3) (3GF), and in 1 set of experiments also 400 nM Triciribine (t; Thermo Fisher) or dimethyl sulfoxide (d; Sigma). Cells were tracked over 7 days for survival (high refractility) and incidence of division(s).

Cell-capture and cyclic-immunofluorescence tracking

Freshly isolated *CD49f*$^+$ or CD34$^+$CD38$^-$ cells were sorted either directly into 384-well streptavidin-coated plates (Thermo Fisher) pretreated with 1 μg/mL α-CD44–biotin[42] (Biolegend), or transferred after a 24- to 64-hour exposure to SFM + 100% or 1% of the 3GF cocktail and 10 μM 5-ethynyl-2′-deoxyuridine (EdU) in 96-well plates. Cells were then fixed, permeabilized, stained, and fluorescently imaged. Fluorescent antibodies used in the first round of imaging were quenched before subsequent rounds of staining and imaging.[43]

Phosphoflow cytometry

CD34$^+$ cells were cultured in SFM for 3 hours either without additional GFs or with 3GF added during the last 5, 15, or 30 minutes. Cells were then immediately fixed, permeabilized, and each time point labeled with different concentrations of a Pacific Blue succinimidyl ester dye (Thermo Fisher), after which cell were combined, stained, and analyzed on a FACSymphony.

Data analysis

Data analysis and statistical tests were performed in R using publicly available packages unless otherwise specified. Statistical tests and significance levels are indicated for each data set.

Results

Human *CD49f*$^+$ cells from CB and adult BM sources display similar clonogenic frequencies in vitro but with an age-associated delay in the kinetics of their outputs

Cell outputs of single *CD49f*$^+$ cells from CB and adult BM were first assessed over an 8-week period in stromal cocultures that support differentiated NM outputs exclusively (Figure 1A; supplemental Figure 1A). The results showed that ~50% of the *CD49f*$^+$ cells from all sources were persistent and produced clones of ≥50 refractile cells detectable at the end of 8 weeks (Figure 1B; pairwise *t* tests $P > .05$). However, the *CD49f*$^+$ cells from the older donors produced fewer early-appearing but ultimately transient clones (pairwise Fisher exact test, $P < .001$; Figure 1C; supplemental Table 2) and their persistent clones became initially detectable at later time points (Figure 1D; pairwise Komolgerov-Smirnov tests, all $P < .0001$). Index sorting data confirmed higher levels of CD33, CD34, and CD90 expression on the most proliferative *CD49f*$^+$ CB cells[23] (supplemental Figure 1B). However, this was not maintained on *CD49f*$^+$ cells from adult sources. Altogether, these findings suggest an age-associated change in mechanism(s) regulating the kinetics of *CD49f*$^+$ cell–output responses to mitogenic stimuli that support their proliferation and NM outputs.

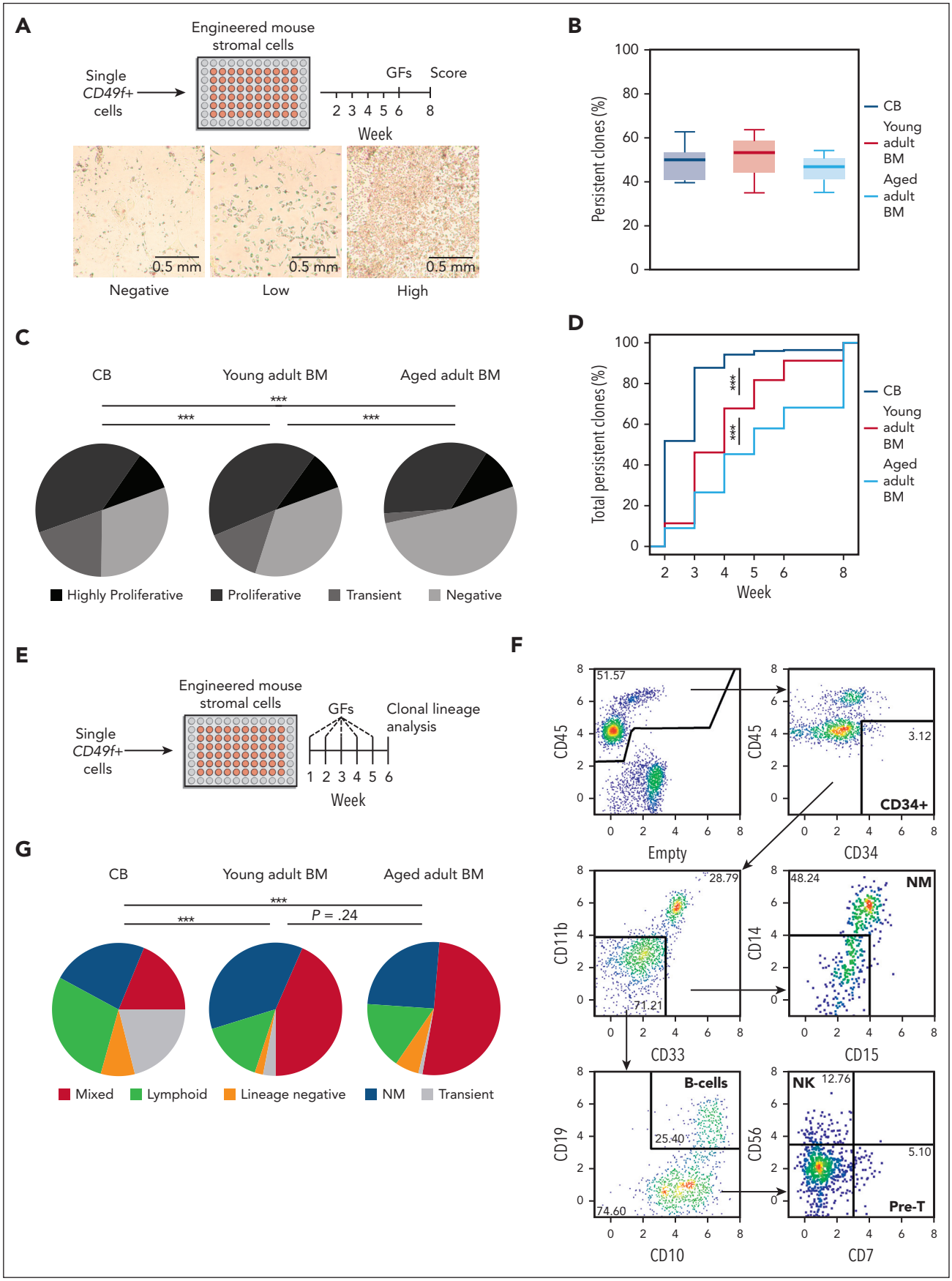

Figure 1.

We then asked if and how aging might affect the timing and cell outputs from single *CD49f*$^+$ cells in a 6-week stromal coculture system (Figure 1E; supplemental Table 4) that efficiently supports NM and B-lymphoid differentiation from CB *CD49f*$^+$ cells in ratios similar to the clonal outputs of this population in immunodeficient mice that had undergone transplantation.[23] In this second in vitro assay, a high frequency of the *CD49f*$^+$ cells from all age groups produced persistent clones (28%-55%, supplemental Table 5). However, the frequency of transient clones produced from the oldest donor–derived *CD49f*$^+$ cells compared with that from CB cells was again markedly reduced (21% vs 1%, Figure 1F-G; supplemental Figure 2A-C; pairwise Fisher exact tests, $P < 5 \times 10^{-8}$). Moreover, persistent clones from the oldest donors of *CD49f*$^+$ cells also appeared later than those from CB (supplemental Figure 2D; pairwise Komolgerov-Smirnov tests, $P = 6.9 \times 10^{-6}$), also suggesting an age-associated blunting of the mitogenic responsiveness of aging human *CD49f*$^+$ cells.

Adult BM but not CB *CD49f*$^+$ cells display enhanced repopulating activity when cotransplanted with CD34$^+$ CB cells

Preliminary transplants of *CD49f*$^+$ cells from normal CB and adult BM into sublethally irradiated immunodeficient mice (supplemental Table 6) confirmed previously reported lower levels of repopulation by adult sources.[22,26] However, the finding of their similar clonogenic frequencies in supportive in vitro systems (Figure 1) suggested that the conventional xenotransplant assay might provide a suboptimal stimulatory environment for eliciting the intrinsic output potential of adult human *CD49f*$^+$ cells. To test this possibility, we cotransplanted 10^4 FACS-purified GFP-labeled CB CD34$^+$ cells together with each test inoculum of 300 nontransduced *CD49f*$^+$ cells to allow distinction of their respective progeny (Figure 2A; supplemental Tables 7 and 8). The contributions of the tested *CD49f*$^+$ cells to the total detectable human, and separated B-lymphoid, NM, and erythroid lineages, and the CD34$^+$ cell compartment were highly variable and no significant age-associated differences in the ratio of their progeny were detected, although only 2 donors per age group were tested (Figure 2B-D; pairwise *t* tests $P > .05$). T cells were not detected in the BM of any of these mice within the first 20 weeks after transplant, although low levels of human T cells were detected in some mice at week 30 after transplant, when the experiments were terminated. The low frequency of emergent GFP$^-$ human cells in samples from mice that had received only GFP-transduced cells, and ddPCR analyses of FACS-purified human GFP$^+$ and GFP$^-$ cells from mice transplanted with both nontransduced *CD49f*$^+$ cells and GFP-transduced CB CD34$^+$ cells indicated that the outputs attributed to the *CD49f*$^+$ cells contained negligible contamination from the cotransplanted GFP$^+$ CB cells (supplemental Figure 2B-F).

We then asked whether the cotransplanted GFP$^+$ CB cells had differentially influenced the outputs of the *CD49f*$^+$ cells from any of the donor sources tested (Figure 2E). Despite the limited donors compared, analyses showed a significant positive correlation exclusively between the outputs attributable to the input *CD49f*$^+$ cells from the young and aged adult donors and the progeny of the cotransplanted GFP$^+$ CB cells but not for the *CD49f*$^+$ CB cells.

CD49f$^+$ cells display a progressive age-related delay in their GF-stimulated division kinetics in vitro

Next, we asked whether the delayed clone development in vitro exhibited by *CD49f*$^+$ cells from adult donors (Figure 1D) would be evident in their initial mitogenic responses. Accordingly, we tracked the behaviors of single *CD49f*$^+$ cells for 7 days in SFM + 3GF (Figure 3A; supplemental Table 9). All sources of these cells showed high levels of survival, with those from CB and the young adults being slightly higher than those from the aged adults (85% vs 72%, log-rank test $P < .001$; Figure 3B; supplemental Figure 4A). However, the time preceding the first division of the viably maintained cells demonstrated a highly significant and progressive increase with increasing donor age (increasing from 57 to 90 hours; Figure 3C; supplemental Figure 4B; all pairwise Holm-corrected, $P < 1 \times 10^{-23}$). Notably, this age-associated delay in the initial mitogenic response of isolated *CD49f*$^+$ cells was not restricted to the first division but was followed by similarly lengthened times to complete a second and third division (Figure 3D-E). Least absolute shrinkage and selection operator (LASSO) regression models from the initial index sorted data showed that only CD38 and cell-size (forward-scatter area) values were consistently negatively associated with the first division timing across all examined groups (supplemental Figure 4C). Taken together, these findings are consistent with the expectation of an early postnatal alteration in the cycling dynamics of HSCs[27,32,33,44,45] and suggest progressive aging-associated alterations to the regulation of their cell cycle kinetics.

CD49f$^+$ cells display a progressive age-related elongation of their G_1 phase

To examine which cell cycle phase(s) in adult *CD49f*$^+$ cells were affected, we used a cell-capture cyclic immunofluorescence approach[42,43] that allowed time-dependent changes in 7 features to be quantified over several measurements on the same individual cells (ie, their DNA content and levels of CD45, CDK2, CDK6, Ki67, pRb, and EdU). This assessment was performed on a combined total of >10 000 cells from 3 samples each of CB, young adult BM, and aged adult BM (supplemental Table 10) cultured in SFM supplemented with high (100%) or low (1%) concentrations of 3GF (Figure 4A-B). This method retained >80% of the initially analyzed cells after 2 additional

Figure 1. Sustained long-term and multilineage output potential of *CD49f*$^+$ cells from birth to late adulthood in clonal in vitro assays. (A) Design of the stromal cell coculture system used to measure the 8-week clonal kinetics of NM cell production from individual human *CD49f*$^+$ cells obtained from differently aged donors. (B) Proportion of individually assessed *CD49f*$^+$ cells that showed persistent outputs to week 8 based on analyses of 898 cells from 5 CB samples, 538 BM cells from 3 young adult donors, and 539 BM cells from 3 samples of aged adult donors. (C) Distribution of clonal outputs from each donor age group (clone categories: H, highly proliferative; P, proliferative; T, transient; N, negative; ***$P < .001$; Fisher exact test). (D) Cumulative distribution of the time at which each persistent clone first appeared (***$P < .001$; Komoglerov-Smirnov test). (E) Design of the stromal coculture system used to measure the 6-week multilineage (lymphoid and/or NM) cell output potential of individual *CD49f*$^+$ cells obtained from differently aged donors. (F) Representative gating strategy of indicated lineages present in the 6-week harvests of the multilineage cocultures described in panel E. (G) Average distribution of the 6-week clone types obtained from the different sources of *CD49f*$^+$ cells tested, based on analyses of 239 cells from 2 CB samples, 240 cells from 2 young adult BM samples, and 240 cells from 2 aged adult BM samples; ***$P < .001$; Fisher exact test.

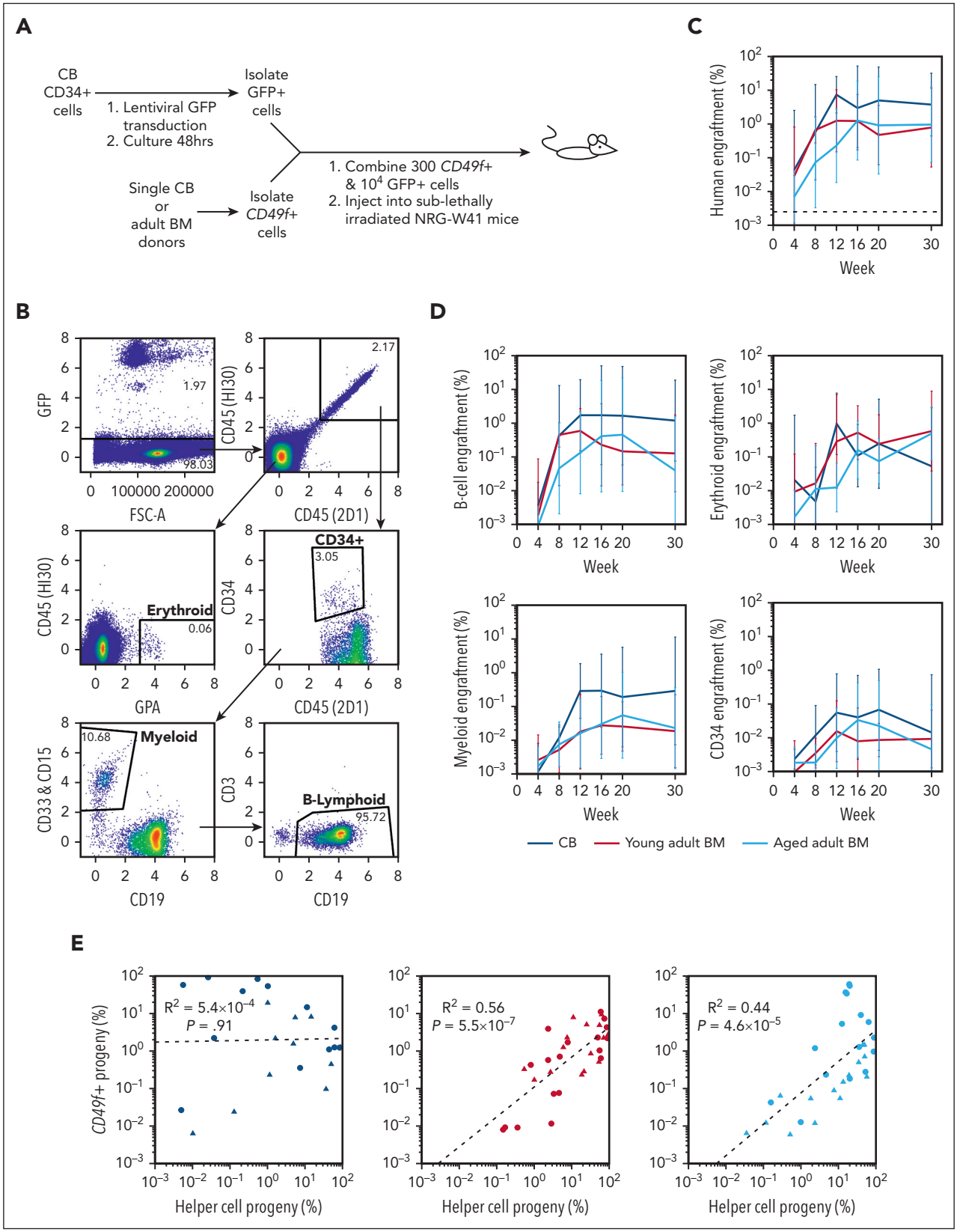

Figure 2. Similar in vivo repopulating activity of neonatal and adult *CD49f*$^+$ cells when cotransplanted with CD34$^+$ CB "helper" cells. (A) Design of a cotransplantation strategy to compare the regenerative potential of *CD49f*$^+$ cells isolated from donors of different ages. (B) Flow-cytometric analysis of the cells in a representative BM aspirate obtained from a mouse that had undergone cotransplantation 12 weeks earlier with CB *CD49f*$^+$ cells and GFP-labeled CD34$^+$ CB cells. (C-D) Percentage of human *CD49f*$^+$ cell (GFP$^-$) (C), and NM, B-lymphoid, erythroid, and CD34$^+$ progeny (D) from input CB, young adult BM, or aged adult BM measured in the total number of viable cells present in the BM aspirate obtained at each time point assessed. Values indicate the geometric mean of pooled values from all mice in each group assessed in 2 independent

rounds of imaging and analysis (supplemental Figure 5A-C). Visualization of the cell cycle progression kinetics of the tracked cells was then achieved by reducing the fluorescence data to a 2D format using the UMAP algorithm[46,47] and separating the data into 3 regions using K-means clustering representative of different phases of the cell cycle (Figure 4C).

The proportion of cells in each of these regions was then determined at each time point for each culture condition analyzed to compare the cell cycle progression of *CD49f*$^+$ and CD34$^+$CD38$^-$ cells from all 3 sources (Figure 4D; supplemental Figure 5D; supplemental Table 11). As expected from their initial quiescent state,[48,49] the majority of the freshly isolated *CD49f*$^+$ and CD34$^+$CD38$^-$ cells (supplemental Figure 6A) were in the G_0 region of the UMAP distribution. However, within 24 hours of exposure to the 100% 3GF cocktail, ~70% of all the CB and young adult BM *CD49f*$^+$ cells but only 50% of aged adult BM cells had transitioned into G_1. After 42 hours, the majority of CB *CD49f*$^+$ cells had progressed into S/G_2/M phase. In contrast, most of the cells obtained from young or aged adults were still in G_1 (Holm-corrected Wilcox tests, $P = 1.7 \times 10^{-9}$ and $P = 2.9 \times 10^{-10}$, respectively) in which they remained for at least another 8 hours (Holm-corrected Wilcox tests, $P = 5.7 \times 10^{-6}$ and $P = 7.3 \times 10^{-7}$; Figure 4D). Baseline levels of CDK6 were markedly lower in the aged adult BM cells (Holm-corrected Wilcox tests $P < 1.4 \times 10^{-13}$) and remained lower for 24 hours. Levels of Ki67, pRb, and CDK2 (a regulator of the G_1 phase to S phase transition), were all lower in the adult *CD49f*$^+$ cells after 42 to 50 hours (Figure 4E). However, after 64 hours in culture, most of the adult *CD49f*$^+$ cells had transitioned into S/G_2/M, indicative of a total prolongation of their first cell cycle transit time of ~14 to 22 hours, in agreement with our independent direct visualization experiments (Figure 3C).

Taken together, these results indicate that the prolonged first division timing in young adult *CD49f*$^+$ cells compared with CB *CD49f*$^+$ cells can be explained primarily by an increased duration of G_1 rather than an increased time required to exit G_0. However, *CD49f*$^+$ cells from aged donors remained in G_0 and G_1 for prolonged periods of time. Interestingly, similar altered cell cycle progression kinetics were exhibited by the CD34$^+$CD38$^-$ cells from the same donors (supplemental Figure 6), suggesting the aging-related prolonged cell cycle transit features persist into the more differentiated cells present in the CD34$^+$CD38$^-$ subset.

Exposure to reduced GF concentrations exaggerates the age-related elongation of G_1 in *CD49f*$^+$ cells

Given that progression into, and through, G_1 relies on mitogenic stimulation,[50-52] we examined how reduced GF stimulation impacts *CD49f*$^+$ cell proliferation. This showed that *CD49f*$^+$ cell survival was maintained at high levels (>75% of maximum) for all cell sources, even at the low concentration of 1% 3GF

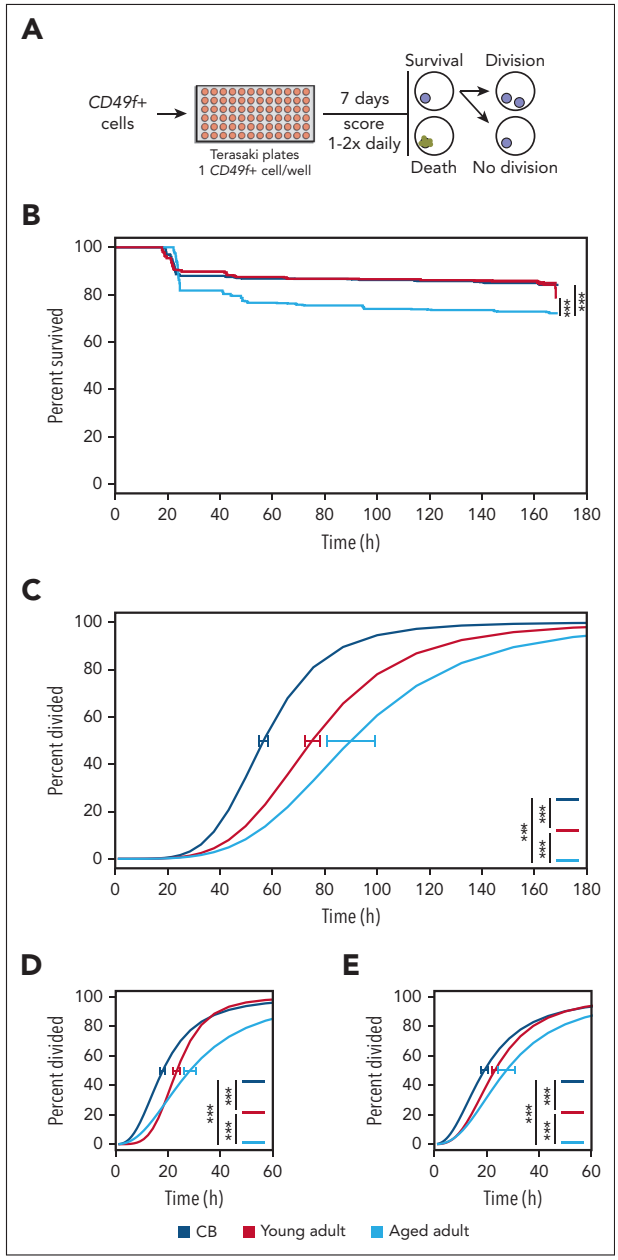

Figure 3. GF-stimulated *CD49f*$^+$ cells display a progressive age-related delay in vitro. (A) Design of the culture system used to compare the survival and cell division kinetics of *CD49f*$^+$ cells isolated from differently aged donors over 7 days of culture. (B) Kaplan-Meier curves of *CD49f*$^+$ cell survival in the cultures described in panel A (log-rank test, ***$P < .001$). (C) Weighted dose-response curves describing the completion of a first division of the different sources of *CD49f*$^+$ tested. Curves reflect only *CD49f*$^+$ cells that remained viable past a first division, or until the end of the assay without dividing. Error bars are indicated at the median point of each curve (CB = 57 hours, young adult = 75 hours, aged adult = 90 hours) and indicate the range defined by ± 1 SEM of this estimate (***$P < .001$). Time required for clones to complete a second (D) or third (E) division after completing their previous division (***$P < .001$).

Figure 2 (continued) experiments (2-3 mice per donor per experiment). Bars indicate the geometric means ± 1 standard error of the mean (SEM). (E) Linear regression analyses of *CD49f*$^+$-progeny (GFP$^-$) and GFP$^+$ chimerism levels for CB (left), young adult BM (center), and aged adult BM (right). Points indicate paired results within each individual mouse at each different time point assessed after transplant. Symbols indicate mice that had undergone transplantation with different donors of the *CD49f*$^+$ cells tested.

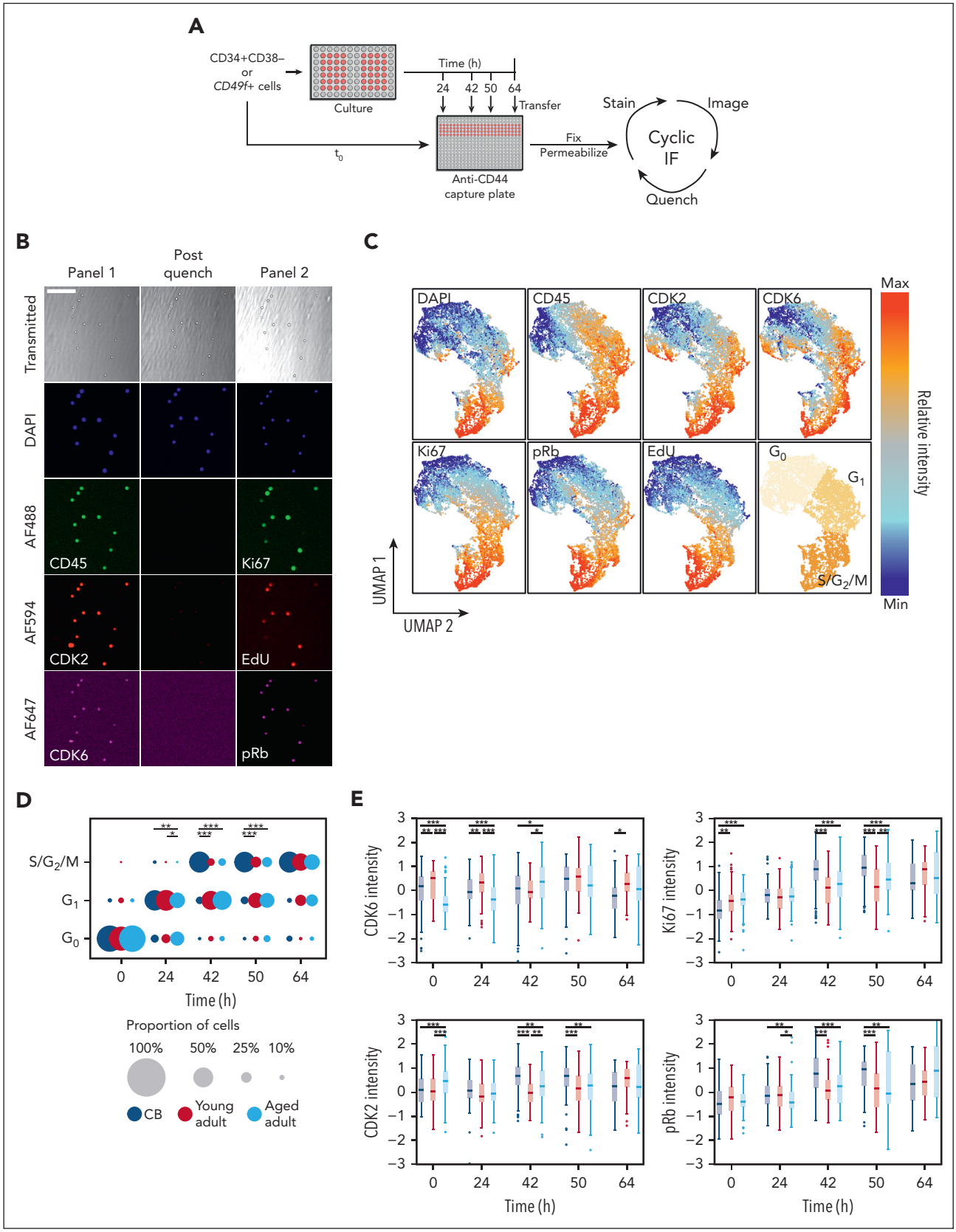

Figure 4. Paired cell cycle state and molecular analysis of individually tracked primitive human hematopoietic cells reveal an age-associated prolongation of G_1 in the adult cells. (A) Experimental design to enable the in vitro serial immunofluorescence tracking of changes in the properties of individual cells isolated from donors of different ages over time. (B) Representative fluorescence images obtained from the experimental design described in panel A; scale bar = 100 μm. (C) UMAP distribution of different phenotypic properties of individually assessed *CD49f*$^+$ and CD34$^+$CD38$^-$ cells from CB and young or aged adult BM cultured for 0, 24, 42, 50, or 64 hours and analyzed as described in panel A. Assignment of regions of the UMAP distribution to the different phases of the cell cycle by K-means clustering (bottom-right). (D) Proportion of *CD49f*$^+$

cocktail, but then steeply decreased thereafter (Figure 5A top panel; supplemental Figure 7A). In contrast, the 3GF concentration required to stimulate *CD49f*$^+$ cells to divide at least once within 7 days was 3 to 5 fold higher for adult cells than for CB cells (CB vs young adult, $P = 1.7 \times 10^{-5}$; and CB vs aged adult, $P = 1.5 \times 10^{-17}$; Figure 5B bottom panel), although the difference between young and aged adult *CD49f*$^+$ cells was not significant ($P = .13$). The clone sizes measured after 7 days were heterogeneous for all sources of *CD49f*$^+$ cells, but the CB-derived clones were consistently larger than those derived from the adults (Holm-corrected pairwise Kruskal-Wallis tests, $P < 1 \times 10^{-17}$; Figure 5B). Furthermore, the *CD49f*$^+$ cells that were able to divide in response to 1% 3GF demonstrated progressive age-related delays in their timing to complete a first division compared with that exhibited in response to 100% 3GF (ie, delayed by 1.3 fold in CB *CD49f*$^+$ cells extending to 1.5 fold and 1.7 fold for the young and aged *CD49f*$^+$ cells, respectively; Figure 5C; supplemental Figure 7B).

To determine the specific phases of the cell cycle affected by culture in 1% 3GF, the proportions of cells from all 3 sources of *CD49f*$^+$ cells present in the different regions of the 2D UMAP distribution were examined (Figure 4C) and compared (Figure 5D; supplemental Table 12). This showed that the majority of young adult *CD49f*$^+$ cells (like their CB counterparts) cultured in 1% 3GF entered G_1 within 24 hours but, unlike the CB *CD49f*$^+$ cells, had not transitioned into $S/G_2/M$ even after 64 hours. Under the same conditions, the aged adult *CD49f*$^+$ cells also showed a delayed entry into, as well as out of, G_1. The extended G_1 in the adult cells was reflected by reduced levels of CDK2, pRb, and Ki67, between 42 and 64 hours (Figure 5E). In addition, after 64 hours, approximately one-third of the young and aged adult *CD49f*$^+$ cells continued to remain in G_0 compared with only approximately one-tenth of the CB *CD49f*$^+$ cells (Figure 5D), the majority of which would be predicted to remain undivided for at least 7 days (Figure 5A, bottom panel). Similar trends were again seen in the coexamined $CD34^+CD38^-$ subset but more of the adult cells transitioned into $S/G_2/M$ within 64 hours (supplemental Figure 7C-D). Taken together, these findings indicate that a reduced 3GF stimulus, which can maintain the viability of a range of CB and adult primitive human hematopoietic cells, is differentially sufficient to induce their exit from G_0 and passage through G_1 in an age- and state-specific fashion.

Adult *CD49f*$^+$ cells display selectively reduced activation of AKT by 3GF

To explore the mechanistic basis of these aging-associated GF-mediated effects on cell cycle progression, we examined several signaling responses previously shown to be activated by a similar GF cocktail (Figure 6A).[38] The relative median shift of specific signaling pathway intermediates at each stimulation time point was compared with that of the corresponding unstimulated fraction contained within the same analyzed sample (supplemental Figure 8A-B). *CD49f*$^+$ cells from all sources displayed robust activation of AKT and STAT5 from 3GF stimulation (Figure 6B; supplemental Figure 8C-D; bootstrapped P values < .05). However, the activation of the AKT response in the *CD49f*$^+$ cells was consistently reduced and shorter in the adult cells, with a continued decline between the young and aged adult cells (similar AKT responses were also seen in the $CD34^+CD38^-CD45RA^-$ fraction; supplemental Figure 8E). Activation of ERK1/2 and β-catenin was also observed but only in CB cells within the times assessed.

To further test the biological importance of this differentially reduced activation of AKT in primitive cells from donors of increasing age, we compared the effect of Triciribine (an AKT inhibitor) on CB and adult *CD49f*$^+$ cells cultured in SFM + 10% 3GF (supplemental Table 15). This showed strong but relatively equal reductions in the survival of all 3 sources (Figure 6C, paired *t* tests, $P < .05$). However, only the surviving adult *CD49f*$^+$ cells showed a decreased ability to divide (Figure 6D, paired *t* tests, $P < .05$). However, the time taken to complete a first division was only marginally extended (1.1-fold, $P < 1.0 \times 10^{-4}$, CB and young adult; 1.2-fold, $P = 4.6 \times 10^{-3}$, aged adult) in all groups with subsequent division cycles also minimally extended (supplemental Figure 9). Taken together, these results point to a selectively pronounced aging effect on the control of AKT signaling in GF-activated human HSCs that differentially affects their proliferative responses.

Discussion

This study presents new evidence of a negative effect of aging on the intrinsic mitogenic response properties of the *CD49f*$^+$ subset of $CD34^+$ human hematopoietic cells, a phenotype shown to highly enrich for cells with long-term in vivo repopulating activity.[21,23-25] A key result was the progressively increased donor age–associated delay in the ability of these initially quiescent cells to enter and advance through the cell cycle under a wide range of stimulatory conditions. These conditions included several in vitro systems with and without stromal cells that allowed the detection of only mature NM cells or also erythroid and B-lineage outputs from single input cells. Evidence of a reduced GF responsiveness of the *CD49f*$^+$ cells from both young and aged adult human donors was also suggested by the selective dependence of their 30-week repopulating activity on a coinjected transplant of $CD34^+$ CB cells.

Interestingly, in both the clonal in vitro assays and bulk in vivo assays able to detect both B-lymphoid and NM potential, it was surprising to detect no evidence of the relative reduction in B-lymphoid output reported in previous studies on aging mice[11-13,35,53] and humans.[18,20] This discrepancy could have several explanations. First, in this study, the cells analyzed were obtained from only 2 samples per age group, with the adult samples originating from BM harvests rather than the CB comparator. Second, the cell outputs examined in the mice that had received transplantation were assessed under more supportive conditions found to be selectively beneficial for adult *CD49f*$^+$ cells achieved using a cotransplant of $CD34^+$ CB cells. In this regard, it is interesting to note that long-term repopulating mouse cells that exhibit only a single mature lineage (platelets)

Figure 4 (continued) cells in different phases of the cell cycle after different times in culture. The size of each circle is scaled to show the proportion of total cells in each cell cycle phase at the culture time point when the assessment was made (*$P < .05$; **$P < .01$; ***$P < .001$; Holm-corrected Wilcox tests). (E) Scaled intensity (Z scores) of CDK6, CDK2, Ki67, and pRb protein levels measured in the *CD49f*$^+$ cells analyzed at each time point shown (*$P < .05$; **$P < .01$; ***$P < .001$; Holm-corrected Wilcox tests).

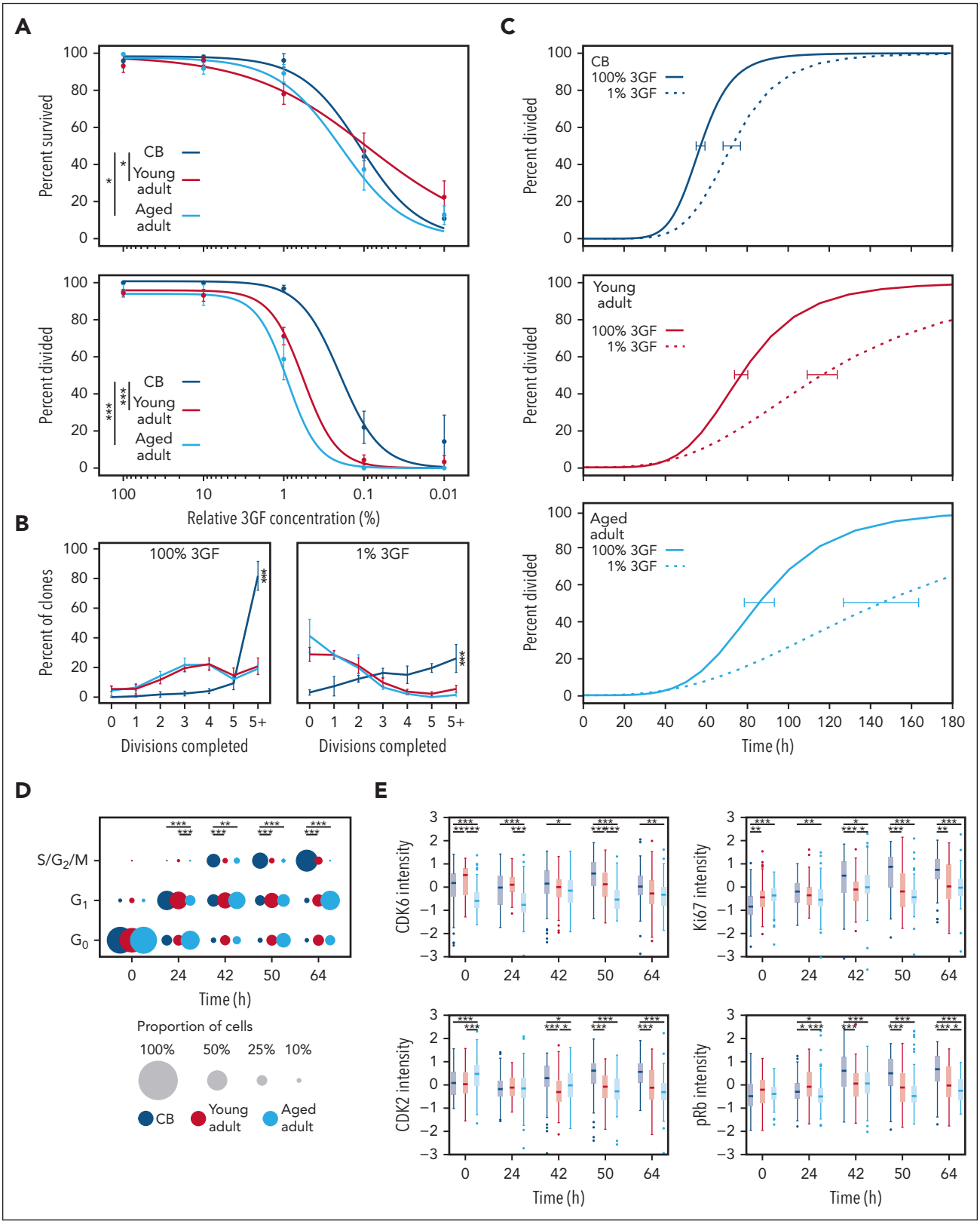

Figure 5. *CD49f*$^+$ cells show an aging-related increase in their 3GF concentration requirement to stimulate their division. (A) Weighted 3GF dose-response curves for *CD49f*$^+$ cell survival (top) and proliferation (bottom) monitored over a 7-day period in vitro as described in Figure 3A. Proliferation curves are normalized to cells that survived either past a first division or for 7 days without dividing. Points indicate the mean ± 1 SEM of the survival and proliferation responses of each group of cell types assessed (*P < .05; ***P < .001). The 50% effective dose concentrations were interpolated from the fitted curves (survival: CB = 0.11%, young adult = 0.09%, aged adult = 0.19%; proliferation: CB = 0.2%, young adult = 0.6%, aged adult = 0.9%). (B) Percent of clones that completed the indicated number of divisions by day 7 at 100% 3GF (left) or 1% 3GF (right). Lines connect the observed mean ± 1 SEM of the proportion of cells from each donor source that had completed the indicated number of divisions within 7 days. (***P < .001; pairwise Kruskal-Wallis tests). (C) Kinetics of 3GF-stimulated timing of a first division of *CD49f*$^+$ cells from different sources exposed to 100% (solid lines) or 1%

long term in vivo, can be stimulated to express a multilineage output rapidly in vitro when appropriately stimulated.[54] Similarly, lymphoid outputs in vivo have been shown to be influenced by extrinsic factors.[55,56] Future efforts to examine the variability of *CD49f*$^+$ cells from different donors of the same age groups and different lineage output assay conditions should help to discriminate the relevance of these different factors.

The age-related delays in *CD49f*$^+$ cell progeny output in the stromal coculture experiments described here were accompanied by a highly apparent delayed timing of the first and subsequent divisions of the initially quiescent *CD49f*$^+$ cells. Taken together, these results suggest an intrinsically determined delay in their GF response mechanism that is established during the aging process and sustained through several division cycles, even as the cells begin to differentiate. Use of a cell-capture and multiplexed molecular phenotyping strategy[42,43] revealed this age-related delay to be because of prolonged G_1 in both young and aged adult cells and a preceding G_0 exit delay observed in only the aged adult cells. The increased baseline levels of CDK6 in the young adult *CD49f*$^+$ cells suggest differential priming of these cells to exit G_0 in response to a mitogen-induced program, because this protein has been demonstrated to affect the kinetics of G_0/G_1 transition in human HSCs.[48] However, baseline CDK6 levels were lower in the aged adult cells than in either the CB or young adult cells, likely contributing to their delayed exit from G_0. CDK2 levels also remained lower for at least 50 hours in adult *CD49f*$^+$ cells, suggesting that the G_1 delay occurs before CDK2 activation that typically follows phosphorylation of Rb by CDK4/6 with cyclin D and inhibition of CDK inhibitors, including p21, p27, and p15.[50,51,57]

This delayed proliferation phenotype was selectively exaggerated under a reduced, nonsaturating GF stimulus, with many adult cells remaining in G_1 for at least 26 hours and an increased proportion failing to exit G_0, resulting in approximately one-third of adult cells remaining viable but undivided for 7 days. These findings suggest a rheostat mode of GF control of both the G_0-to-G_1 and G_1-to-S phase transitions and an aging-associated increase in the stimulation-dependent signaling events required to promote these transitions. In agreement with this model, we found that AKT activation was progressively reduced in both adult *CD49f*$^+$ cells and $CD34^+CD38^-CD45RA^-$ cells compared with their CB counterparts after a strong mitogenic stimulus (Figure 6E). Similarly, inhibition of AKT activity equally reduced survival across the different sources but only reduced the ability of adult *CD49f*$^+$ cells to complete ≥1 divisions with overall lesser impacts on the rate at which divisions were completed. These findings suggest that AKT signaling responses control 2 key activities. The first is whether or not the cell will survive, and the second is whether the cell will proceed into cycle or remain quiescent. The relatively small impact on division timing observed in cells with selectively inhibited AKT suggests that AKT signaling contributes to, but is not solely responsible for, the overall extended proliferation kinetics observed between the different age groups, with the differential activity of other factors then providing a larger impact (Figure 6F). Recent studies have also demonstrated the impact of ERK signaling dynamics and metabolic activation on the immediate progeny of GF-stimulated HSCs, suggestive of a connected mechanism of regulation.[58-60]

Importantly, these findings do not preclude additional delays at other stages of cell cycle progression control, including other points within G_1. Indeed, the finding of decreased mini-chromosome maintenance helicase levels in aged mouse HSCs compared with those of younger adult mice, as well as the increased replication stress experienced by these cells during S phase, suggest that multiple points of cell cycle progression may be affected.[35] A recent report of altered Cdc42 activity as a potential contributor to age-related proliferative delays in primitive human hematopoietic cells adds further weight to this possibility.[17]

Taken together, the demonstration here of a profound and progressive postnatal decline in GF sensitivity of very primitive normal human hematopoietic cells attributed, at least in part, to altered AKT signaling could be relevant to many aspects of human hematopoiesis. These include not only potential effects of aging on mature blood cell outputs,[2-5,7,8] differential induction of long-term repopulating activity under conditions that promote regenerative responses vs established homeostasis, and the ability of clonal hematopoiesis of indeterminate potential clones to gain ascendancy with increasing age.[6]

Acknowledgments

The authors thank M. Hale, G. Edin, D. Wilkinson, and the staff of the British Columbia Cancer Agency Stem Cell Assay Laboratory for technical assistance, including the acquisition and some of the initial processing of CB, mPB, and BM samples.

This work was supported by subawards to C.J.E. from the Terry Fox Foundation Program Project grant #1074 and the Canadian Cancer Society grant #705047. C.A.H. held a CIHR Frederick Banting and Charles Best Doctoral Scholarship and a UBC Graduate Fellowship.

Authorship

Contribution: C.A.H. and C.J.E. designed the experiments and wrote the manuscript; S.W.W. performed the GFP and Y-chromosome ddPCRs and assisted with other experiments; F.W. assisted with the multilineage coculture experiments; M.E.M. assisted with the AKT inhibition experiments; C.A.H. performed experiments, all data analysis, and figure preparation; and all authors read and approved this manuscript.

Conflict-of-interest disclosure: The authors declare no competing financial interests.

Correspondence: Connie J. Eaves, British Columbia Cancer Research Institute, Terry Fox Laboratory 675 W. 10th Ave, Vancouver, British Columbia V5Z 1L3 Canada; email: ceaves@bccrc.ca.

Figure 5 (continued) (dotted lines) 3GF cocktail (CB: 100% and 1% 3GF, 57 hours and 72 hours, respectively; young adult: 100% and 1% 3GF, 77 hours and 116 hours, respectively; aged adult: 100% and 1% 3GF, 85 hours and 145 hours, respectively). Error bars drawn at the median value of each curve indicate the range defined by ± 1 SEM of this estimate for each sample type. (D) Proportion of *CD49f*$^+$ cells cultured in 1% 3GF in different phases of the cell cycle assessed at different times. The size of each circle represents the proportion of total cells in each phase at the time shown (*P < .05; **P < .01; ***P < .001; Holm-corrected Wilcox tests). (E) Scaled intensity (Z scores) of CDK6, CDK2, Ki67, and pRb protein levels found in the *CD49f*$^+$ cells analyzed (*P < .05; **P < .01; ***P < .001; Holm-corrected Wilcox tests).

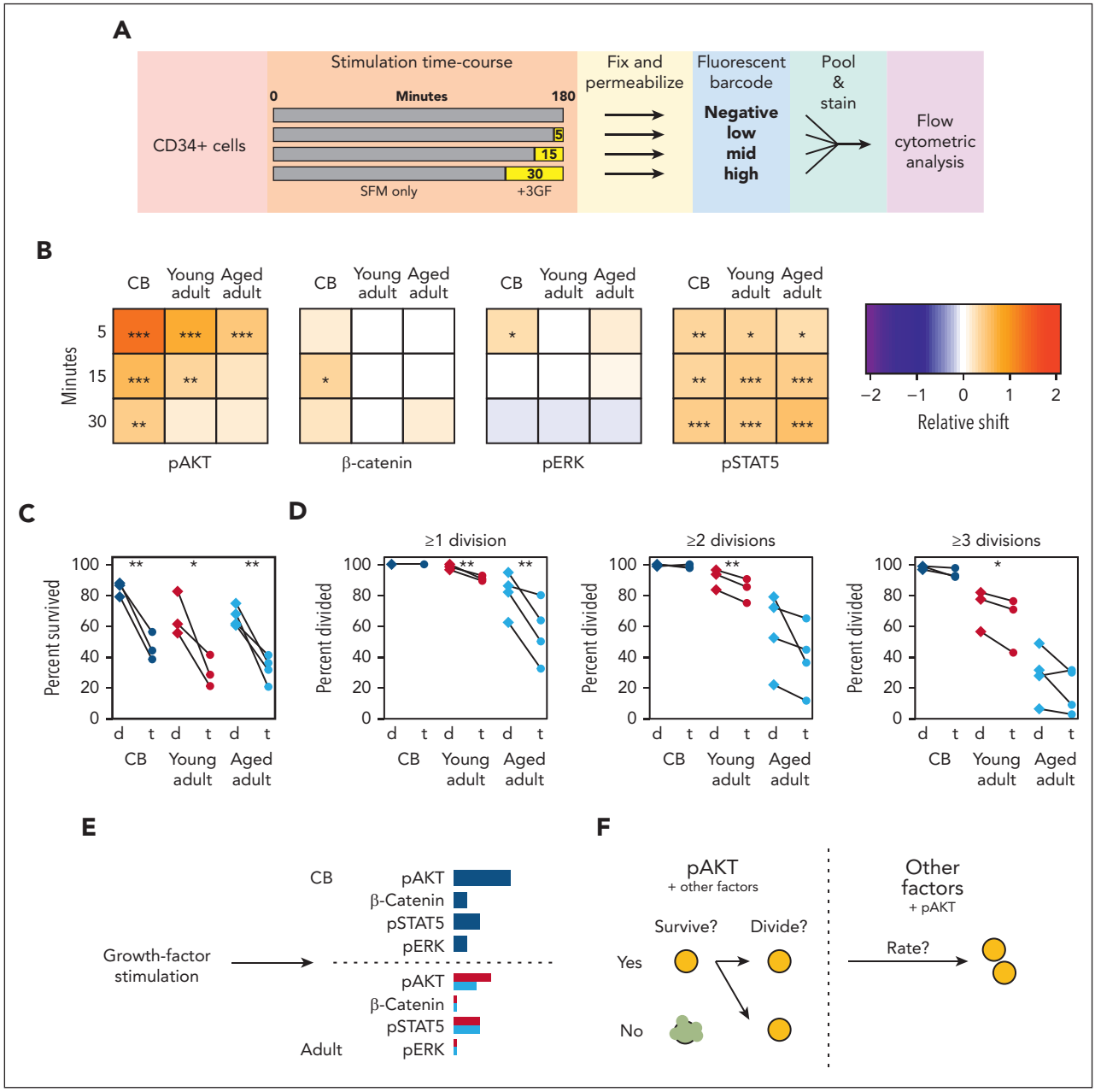

Figure 6. AKT signaling drives the 3GF-activated survival and division of primitive human hematopoietic cells. (A) Experimental design used to compare the 3GF-stimulated time course of signaling protein activation assessed by flow cytometric analysis. (B) Median relative shift in the intensity of the indicated marker from the corresponding unstimulated sample in *CD49f*$^+$ cells exposed to 3GF for different times. Asterisks indicate significant differences from the unstimulated samples (*P < .05; **P < .01; ***P < .001; bootstrapped probabilities). Paired survival (C) and proliferation (D) effects of dimethyl sulfoxide (d)- or triciribine (t)-mediated inhibition of AKT activation. (E) Model of *CD49f*$^+$ pathway activation after short-term 3GF stimulation. The length of the colored bars indicates the relative strength of activation of the indicated marker. CB responses are shown in navy, young adult in red, and aged adult in teal. (F) A model of the role of AKT signaling and other factors in regulating different stages of primitive human hematopoietic cell survival and proliferation.

Footnotes

Submitted 23 May 2022; accepted 13 January 2023; prepublished online on *Blood* First Edition 18 January 2023. https://doi.org/10.1182/blood.2022017174.

Data are available on request from the corresponding author, Connie J. Eaves (ceaves@bccrc.ca).

The online version of this article contains a data supplement.

There is a *Blood* Commentary on this article in this issue.

The publication costs of this article were defrayed in part by page charge payment. Therefore, and solely to indicate this fact, this article is hereby marked "advertisement"in accordance with 18 USC section 1734.

REFERENCES

1. Laurenti E, Göttgens B. From haematopoietic stem cells to complex differentiation landscapes. *Nature*. 2018;553(7689):418-426.
2. Blanco E, Pérez-Andrés M, Arriba-Méndez S, et al. Age-associated distribution of normal B-cell and plasma cell subsets in peripheral blood. *J Allergy Clin Immunol*. 2018;141(6):2208-2219.e16.
3. Comans-Bitter WM, de Groot R, van den Beemd R, et al. Immunophenotyping of blood lymphocytes in childhoodReference values for lymphocyte subpopulations. *J Pediatr*. 1997;130(3):388-393.
4. Geiger H, de Haan G, Florian MC. The ageing haematopoietic stem cell compartment. *Nat Rev Immunol*. 2013;13(5):376-389.
5. Guralnik JM, Eisenstaedt RS, Ferrucci L, Klein HG, Woodman RC. Prevalence of anemia in persons 65 years and older in the United States: evidence for a high rate of unexplained anemia. *Blood*. 2004;104(8):2263-2268.
6. Jaiswal S, Ebert BL. Clonal hematopoiesis in human aging and disease. *Science*. 2019;366(6465):eaan4673.
7. Morbach H, Eichhorn EM, Liese JG, Girschick HJ. Reference values for B cell subpopulations from infancy to adulthood: age-dependent reference values for B cell populations. *Clin Exp Immunol*. 2010;162(2):271-279.
8. Ogawa T, Kitagawa M, Hirokawa K. Age-related changes of human bone marrow: a histometric estimation of proliferative cells, apoptotic cells, T cells, B cells and macrophages. *Mech Ageing Dev*. 2000;117(1-3):57-68.
9. Chin DWL, Yoshizato T, Virding Culleton S, et al. Aged healthy mice acquire clonal hematopoiesis mutations. *Blood*. 2022;139(4):629-634.
10. Mitchell E, Spencer Chapman M, Williams N, et al. Clonal dynamics of haematopoiesis across the human lifespan. *Nature*. 2022;606(7913):343-350.
11. Benz C, Copley MR, Kent DG, et al. Hematopoietic stem cell subtypes expand differentially during development and display distinct lymphopoietic programs. *Cell Stem Cell*. 2012;10(3):273-283.
12. Cho RH, Sieburg HB, Muller-Sieburg CE. A new mechanism for the aging of hematopoietic stem cells: aging changes the clonal composition of the stem cell compartment but not individual stem cells. *Blood*. 2008;111(12):5553-5561.
13. Dykstra B, Olthof S, Schreuder J, Ritsema M, de Haan G. Clonal analysis reveals multiple functional defects of aged murine hematopoietic stem cells. *J Exp Med*. 2011;208(13):2691-2703.
14. Dykstra B, Kent D, Bowie M, et al. Long-term propagation of distinct hematopoietic differentiation programs in vivo. *Cell Stem Cell*. 2007;1(2):218-229.
15. Sanjuan-Pla A, Macaulay IC, Jensen CT, et al. Platelet-biased stem cells reside at the apex of the haematopoietic stem-cell hierarchy. *Nature*. 2013;502(7470):232-236.
16. Yamamoto R, Morita Y, Ooehara J, et al. Clonal analysis unveils self-renewing lineage-restricted progenitors generated directly from hematopoietic stem cells. *Cell*. 2013;154(5):1112-1126.
17. Amoah A, Keller A, Emini R, et al. Aging of human hematopoietic stem cells is linked to changes in Cdc42 activity. *Haematologica*. 2022;107(2):393-402.
18. Kuranda K, Vargaftig J, de la Rochere P, et al. Age-related changes in human hematopoietic stem/progenitor cells: aging of human HSC. *Aging Cell*. 2011;10(3):542-546.
19. Nilsson AR, Soneji S, Adolfsson S, Bryder D, Pronk CJ. Human and murine hematopoietic stem cell aging is associated with functional impairments and intrinsic megakaryocytic/erythroid bias. *PLoS One*. 2016;11(7):e0158369.
20. Pang WW, Price EA, Sahoo D, et al. Human bone marrow hematopoietic stem cells are increased in frequency and myeloid-biased with age. *Proc Natl Acad Sci U S A*. 2011;108(50):20012-20017.
21. Belluschi S, Calderbank EF, Ciaurro V, et al. Myelo-lymphoid lineage restriction occurs in the human haematopoietic stem cell compartment before lymphoid-primed multipotent progenitors. *Nat Commun*. 2018;9(1):4100.
22. Huntsman HD, Bat T, Cheng H, et al. Human hematopoietic stem cells from mobilized peripheral blood can be purified based on CD49f integrin expression. *Blood*. 2015;126(13):1631-1633.
23. Knapp DJHF, Hammond CA, Hui T, et al. Single-cell analysis identifies a CD33 + subset of human cord blood cells with high regenerative potential. *Nat Cell Biol*. 2018;20(6):710-720.
24. Knapp DJHF, Hammond CA, Miller PH, et al. Dissociation of survival, proliferation, and state control in human hematopoietic stem cells. *Stem Cell Reports*. 2017;8(1):152-162.
25. Notta F, Doulatov S, Laurenti E, Poeppl A, Jurisica I, Dick JE. Isolation of single human hematopoietic stem cells capable of long-term multilineage engraftment. *Science*. 2011;333(6039):218-221.
26. Wang K, Guzman AK, Yan Z, et al. Ultra-high-frequency reprogramming of individual long-term hematopoietic stem cells yields low somatic variant induced pluripotent stem cells. *Cell Rep*. 2019;26(10):2580-2592.e7.
27. Bowie MB, Kent DG, Dykstra B, et al. Identification of a new intrinsically timed developmental checkpoint that reprograms key hematopoietic stem cell properties. *Proc Natl Acad Sci U S A*. 2007;104(14):5878-5882.
28. Foudi A, Hochedlinger K, Van Buren D, et al. Analysis of histone 2B-GFP retention reveals slowly cycling hematopoietic stem cells. *Nat Biotechnol*. 2009;27(1):84-90.
29. Morcos MNF, Zerjatke T, Glauche I, et al. Continuous mitotic activity of primitive hematopoietic stem cells in adult mice. *J Exp Med*. 2020;217(6):e20191284.
30. Sawai CM, Babovic S, Upadhaya S, et al. Hematopoietic stem cells are the major source of multilineage hematopoiesis in adult animals. *Immunity*. 2016;45(3):597-609.
31. Wilson A, Laurenti E, Oser G, et al. Hematopoietic stem cells reversibly switch from dormancy to self-renewal during homeostasis and repair. *Cell*. 2008;135(6):1118-1129.
32. Baerlocher GM, Rice K, Vulto I, Lansdorp PM. Longitudinal data on telomere length in leukocytes from newborn baboons support a marked drop in stem cell turnover around 1 year of age. *Aging Cell*. 2007;6(1):121-123.
33. Sidorov I, Kimura M, Yashin A, Aviv A. Leukocyte telomere dynamics and human hematopoietic stem cell kinetics during somatic growth. *Exp Hematol*. 2009;37(4):514-524.
34. Dykstra B, Ramunas J, Kent D, et al. High-resolution video monitoring of hematopoietic stem cells cultured in single-cell arrays identifies new features of self-renewal. *Proc Natl Acad Sci U S A*. 2006;103(21):8185-8190.
35. Flach J, Bakker ST, Mohrin M, et al. Replication stress is a potent driver of functional decline in ageing haematopoietic stem cells. *Nature*. 2014;512(7513):198-202.
36. Hui T, Cao Q, Wegrzyn-Woltosz J, et al. High-resolution single-cell DNA methylation measurements reveal epigenetically distinct hematopoietic stem cell subpopulations. *Stem Cell Reports*. 2018;11(2):578-592.
37. Knapp DJHF, Hammond CA, Wang F, et al. A topological view of human CD34+ cell state trajectories from integrated single-cell output and proteomic data. *Blood*. 2019;133(9):927-939.
38. Knapp DJHF, Hammond CA, Aghaeepour N, et al. Distinct signaling programs control human hematopoietic stem cell survival and proliferation. *Blood*. 2017;129(3):307-318.
39. Notta F, Zandi S, Takayama N, et al. Distinct routes of lineage development reshape the human blood hierarchy across ontogeny. *Science*. 2016;351(6269):aab2116.
40. Velten L, Haas SF, Raffel S, et al. Human haematopoietic stem cell lineage commitment is a continuous process. *Nat Cell Biol*. 2017;19(4):271-281.
41. Miller PH, Rabu G, MacAldaz M, et al. Analysis of parameters that affect human hematopoietic cell outputs in mutant c-kit-immunodeficient mice. *Exp Hematol*. 2017;48:41-49.
42. Loeffler D, Wang W, Hopf A, et al. Mouse and human HSPC immobilization in liquid culture by CD43- or CD44-antibody coating. *Blood*. 2018;131(13):1425-1429.

43. Lin JR, Fallahi-Sichani M, Sorger PK. Highly multiplexed imaging of single cells using a high-throughput cyclic immunofluorescence method. *Nat Commun*. 2015;6(1):8390.

44. Bowie MB, McKnight KD, Kent DG, McCaffrey L, Hoodless PA, Eaves CJ. Hematopoietic stem cells proliferate until after birth and show a reversible phase-specific engraftment defect. *J Clin Invest*. 2006;116(10):2808-2816.

45. Copley MR, Babovic S, Benz C, et al. The Lin28b–let-7–Hmga2 axis determines the higher self-renewal potential of fetal haematopoietic stem cells. *Nat Cell Biol*. 2013;15(8):916-925.

46. Becht E, McInnes L, Healy J, et al. Dimensionality reduction for visualizing single-cell data using UMAP. *Nat Biotechnol*. 2018;37(1):38-44.

47. McInnes L, Healy J, Saul N, Großberger L. UMAP: Uniform Manifold Approximation and Projection. *JOSS*. 2018;3(29):861.

48. Laurenti E, Frelin C, Xie S, et al. CDK6 levels regulate quiescence exit in human hematopoietic stem cells. *Cell Stem Cell*. 2015;16(3):302-313.

49. Wilpshaar J, Falkenburg JHF, Tong X, et al. Similar repopulating capacity of mitotically active and resting umbilical cord blood CD34+ cells in NOD/SCID mice. *Blood*. 2000;96(6):2100-2107.

50. Hume S, Dianov GL, Ramadan K. A unified model for the G1/S cell cycle transition. *Nucleic Acids Res*. 2020;48(22):12483-12501.

51. Sherr CJ. The Pezcoller lecture: cancer cell cycles revisited. *Cancer Res*. 2000;60(14):3689-3695.

52. Sherr CJ. Mammalian G1 cyclins. *Cell*. 1993;73(6):1059-1065.

53. Grover A, Sanjuan-Pla A, Thongjuea S, et al. Single-cell RNA sequencing reveals molecular and functional platelet bias of aged haematopoietic stem cells. *Nat Commun*. 2016;7(1):11075.

54. Carrelha J, Meng Y, Kettyle LM, et al. Hierarchically related lineage-restricted fates of multipotent haematopoietic stem cells. *Nature*. 2018;554(7690):106-111.

55. Ergen AV, Boles NC, Goodell MA. Rantes/Ccl5 influences hematopoietic stem cell subtypes and causes myeloid skewing. *Blood*. 2012;119(11):2500-2509.

56. Young K, Eudy E, Bell R, et al. Decline in IGF1 in the bone marrow microenvironment initiates hematopoietic stem cell aging. *Cell Stem Cell*. 2021;28(8):1473-1482.e7.

57. García-Gutiérrez L, Delgado MD, León J. MYC oncogene contributions to release of cell cycle brakes. *Genes (Basel)*. 2019;10(3):244.

58. Wang W, Zhang Y, Dettinger P, et al. Cytokine combinations for human blood stem cell expansion induce cell-type– and cytokine-specific signaling dynamics. *Blood*. 2021;138(10):847-857.

59. García-Prat L, Kaufmann KB, Schneiter F, et al. TFEB-mediated endolysosomal activity controls human hematopoietic stem cell fate. *Cell Stem Cell*. 2021;28(10):1838-1850.e10.

60. Loeffler D, Wehling A, Schneiter F, et al. Asymmetric lysosome inheritance predicts activation of haematopoietic stem cells. *Nature*. 2019;573(7774):426-429.